

# ASPIDES kickoff meeting

January 30th, 2025

## Bulk damage study in CMOS SPADs

INSIDE project (CSN V)

**Marcello Campajola** (University of Naples 'Federico II' and INFN)

[marcello.campajola@na.infn.it](mailto:marcello.campajola@na.infn.it)



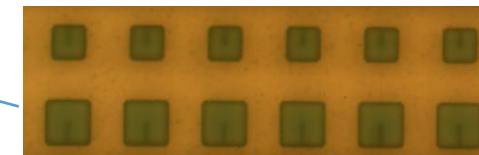
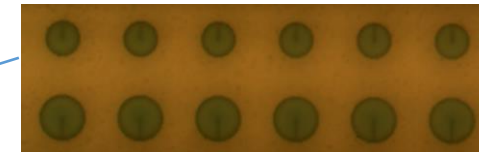
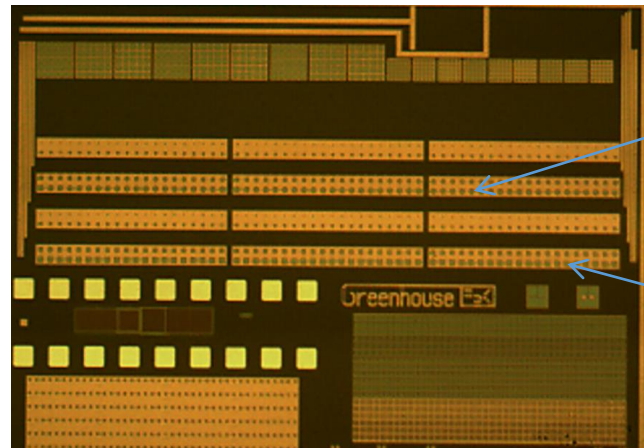
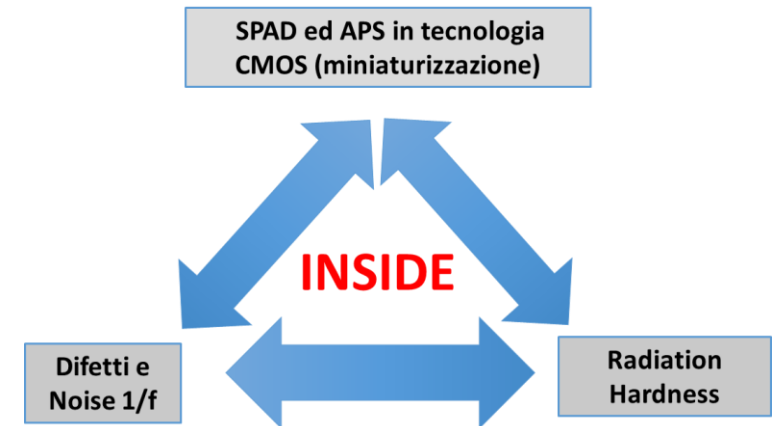
# INSIDE project

## INSIDE: Flicker Noise Studies for Investigation of Detector pErformances

CSNV experiment in 2017-2020, PI: F. Di Capua

Study of radiation induced defects in photosensors

- Partnership with FBK (D. Stoppa)
- Few samples of 150-nm CMOS SPADs test chips



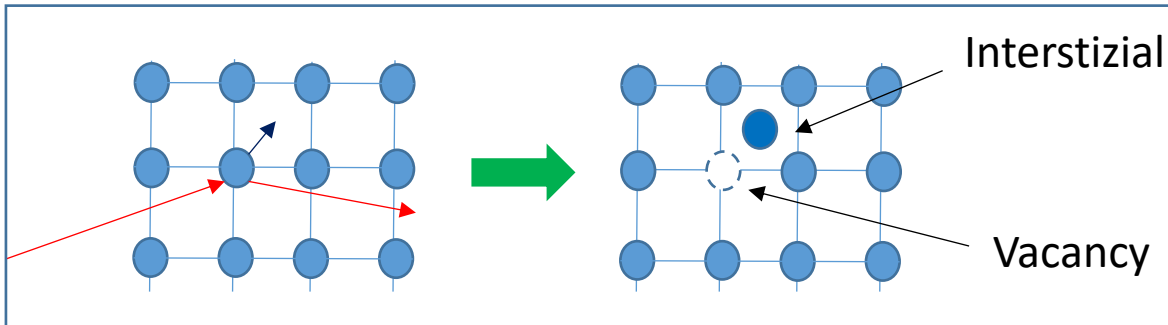
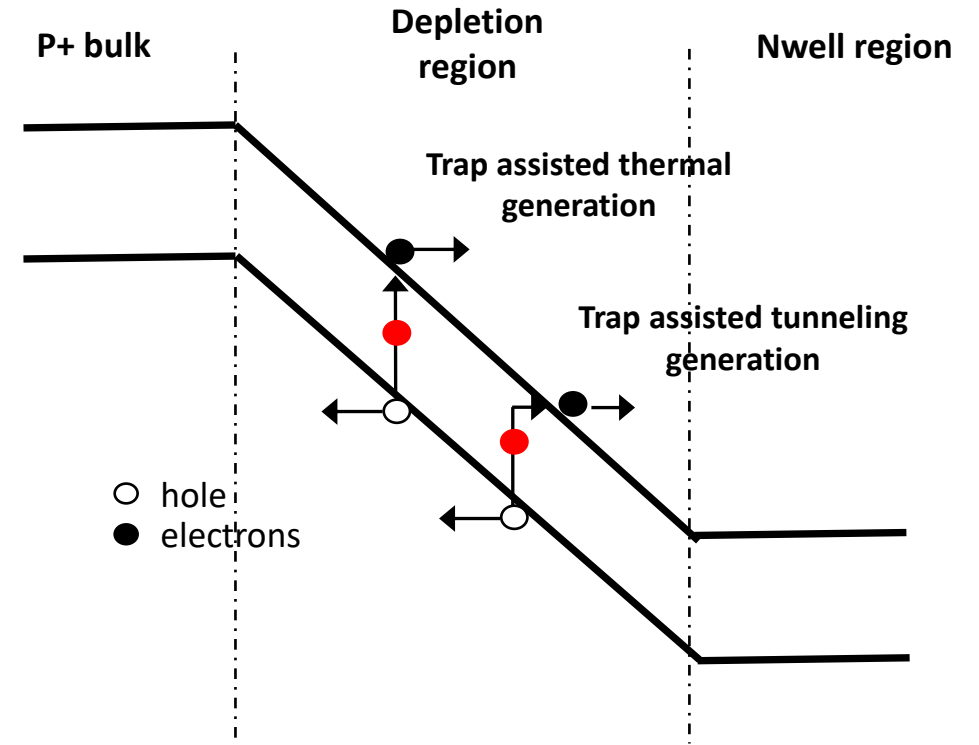
# Dark counts and bulk damage

**Dark Count Rate (DCR)** enhanced by mid-gap energy levels in the depletion region through both

- **Thermal (Shockley–Read–Hall generation);**
- **Tunnelling processes;**

Mid-gap energy levels due to:

- Fabrication process impurities;
- **Radiation induced effects, displacement damage mainly.**



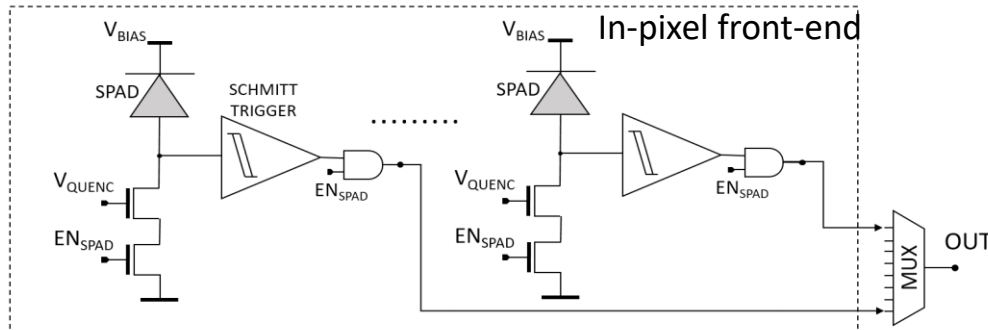
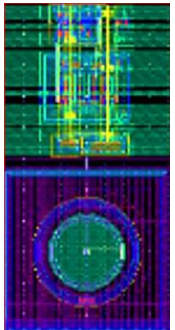
Displacement of Si-atoms from lattice structure due to incident particles.

Typical defects are dopant-related vacancy complexes, as phosphorus-vacancy (P-V), or di-vacancy (V-V) defects.

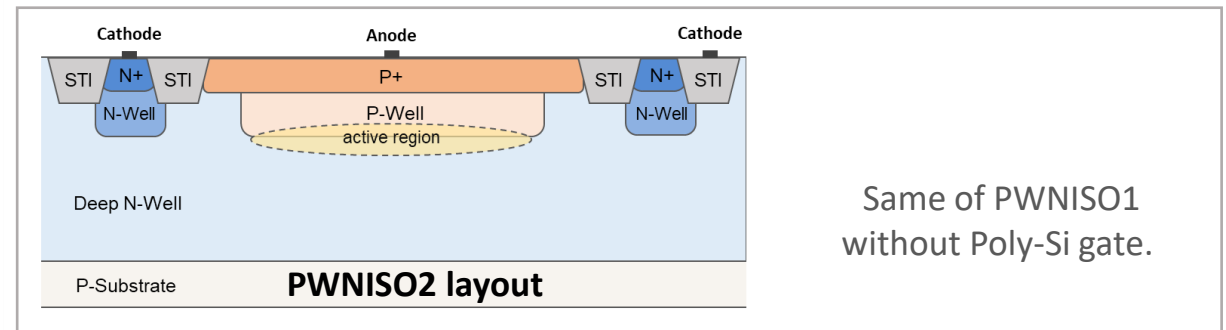
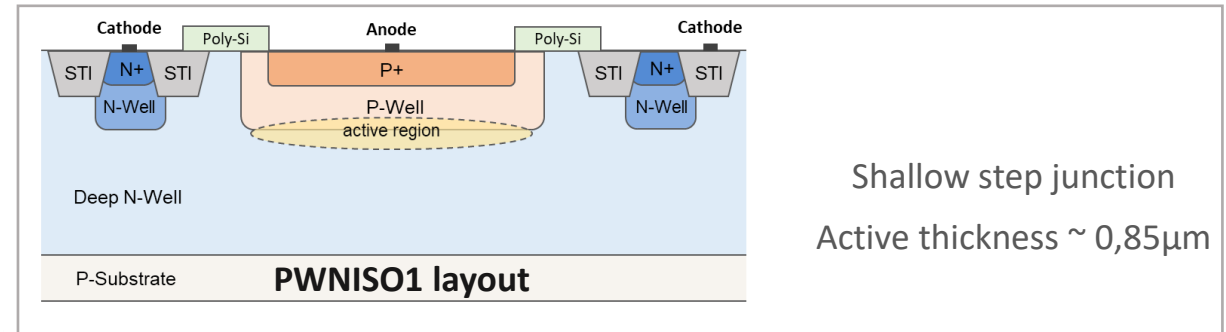
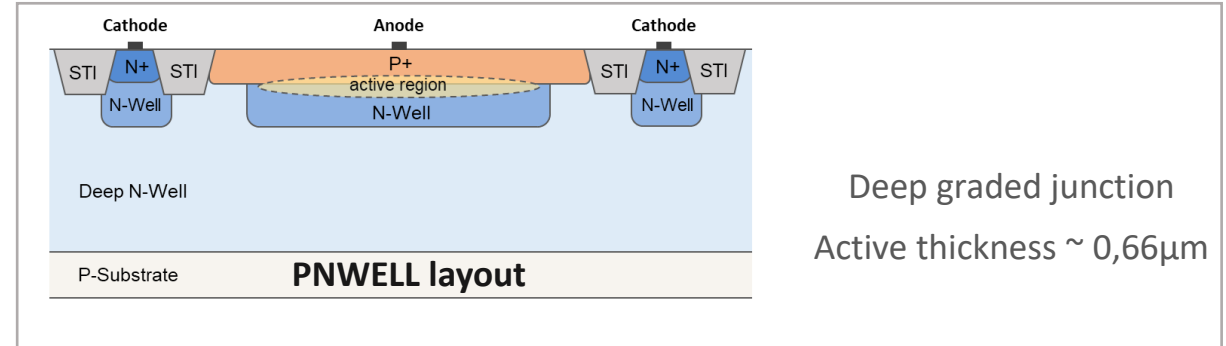
# Devices Under Test

Devices designed by Fondazione Bruno Kessler (FBK) and implemented in a **150-nm CMOS process** [1]:

- **Three junction layouts: PNWELL and PWNISO1/2;**
- **Several active area sizes: 5x5, 10x10, 15x15, 20x20  $\mu\text{m}^2$ ;**
- **Each SPADs is implemented with its front-end electronics:**
  - A trigger to digitalize the pulse;
  - MUX to select one pixel at the time;

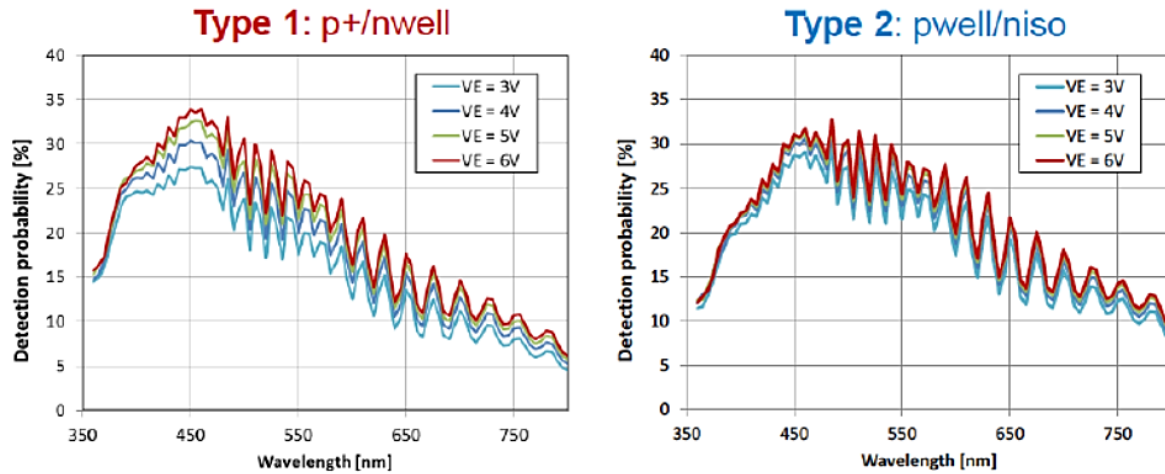


[1] L. Pancheri, D. Stoppa, [Low-noise Single Photon Avalanche Diodes in 0.15  \$\mu\text{m}\$  CMOS Technology](#),



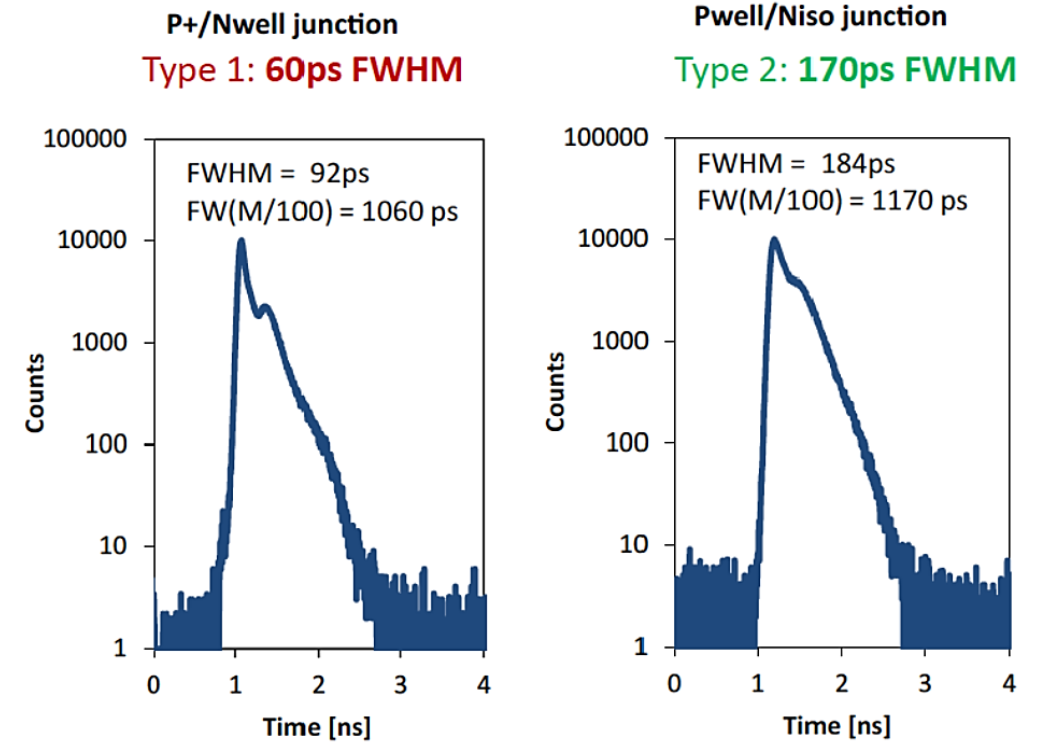
# FBK CMOS SPAD

pde



“Solid-state single-photon Detectors and CMOS Readout Circuits for Positron Emission Tomography Applications”, *Hesong Xu, et. Al.*

Time resolution



“Low-noise Single Photon Avalanche Diodes in 0.15  $\mu\text{m}$  CMOS Technology”, *L Pancheri, D Stoppa*

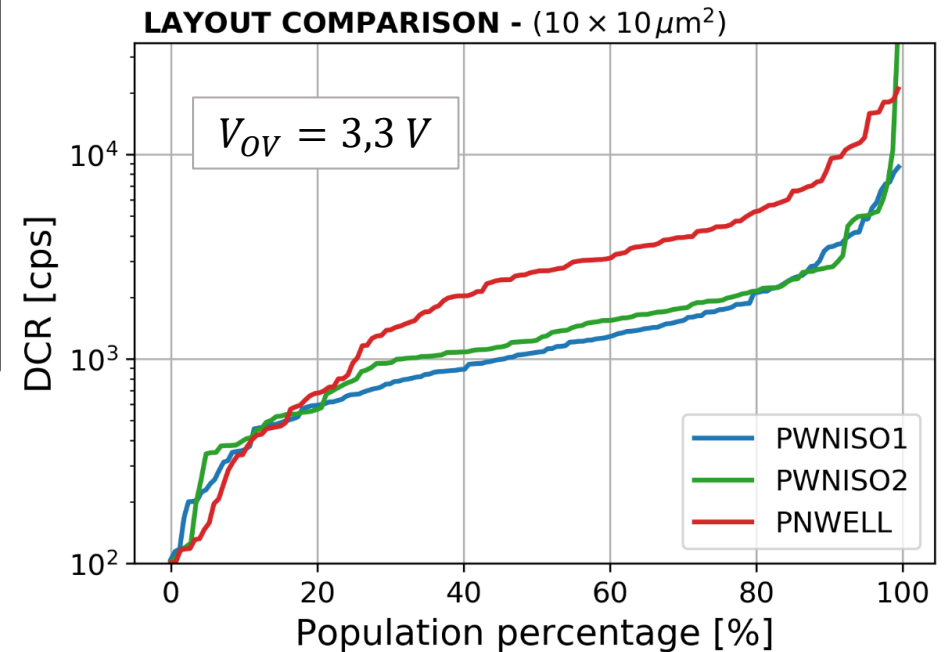
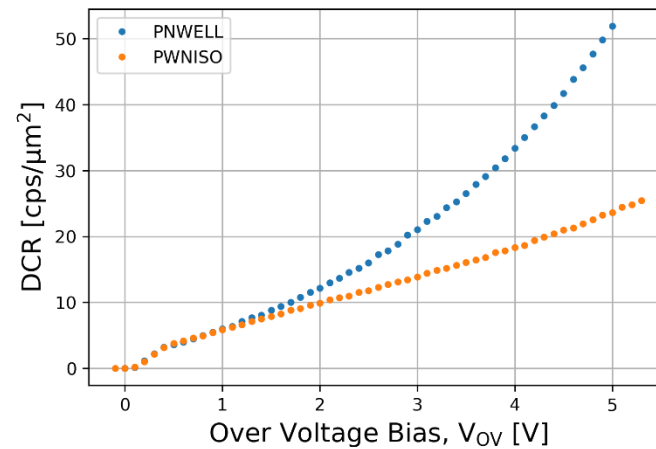
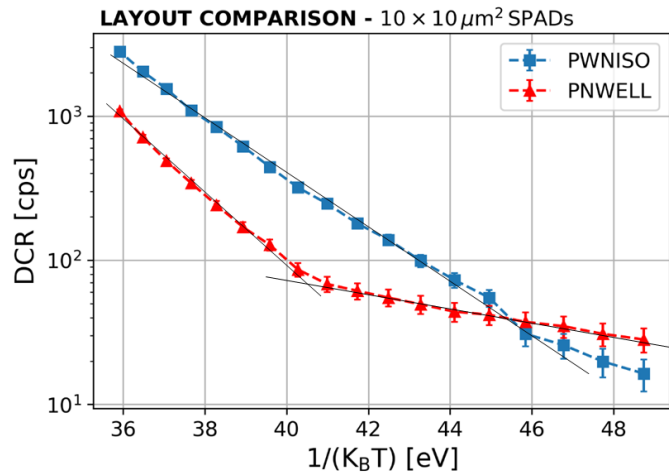
# Pre-irradiation characterization

Device have been characterized before irradiation.

- PNWELL shows a significant tunnelling contribution to the DCR.

$10 \times 10 \mu\text{m}^2$  SPADs

	PNWELL	PWNISO1	PWNISO2
Mean DCR [cps]	~1400	~1700	~3600



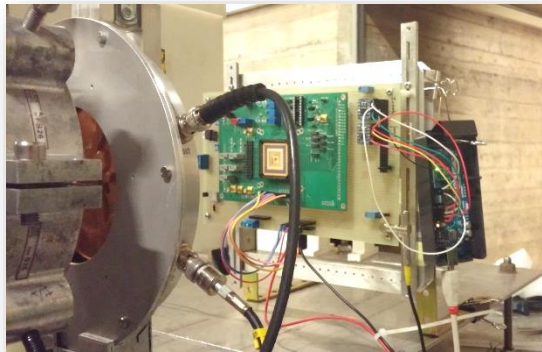
# Irradiation campaigns

Proton test performed at INFN-LNS in Catania (Italy) using:

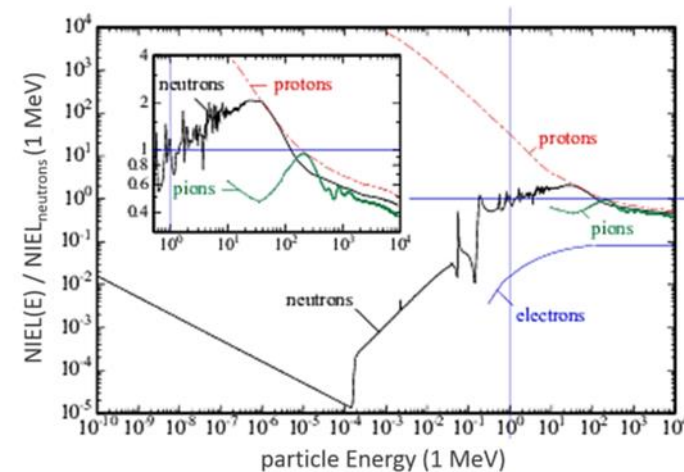
- 16 MeV proton beam;
- Delivered fluences:  $10^{10} - 10^{11} p/cm^2$

Electron test performed at ILU-6 accelerator at the Warsaw Institute of Chemistry and Nuclear Technology:

- 2 MeV electron beam;
- Delivered fluences:  $10^{12} e/cm^2$



particle	Fluence [e/cm <sup>2</sup> ]	TID [krad]	DDD [TeV/g]
$p^+$	$6,7 \cdot 10^9$	2,3	45
$p^+$	$1,4 \cdot 10^{10}$	4,8	94
$p^+$	$2,0 \cdot 10^{10}$	7,1	139
$p^+$	$2,8 \cdot 10^{10}$	9,6	188
$p^+$	$4,1 \cdot 10^{10}$	14	283
$e^-$	$3,48 \cdot 10^{12}$	88	155
$e^-$	$6,92 \cdot 10^{12}$	173	309

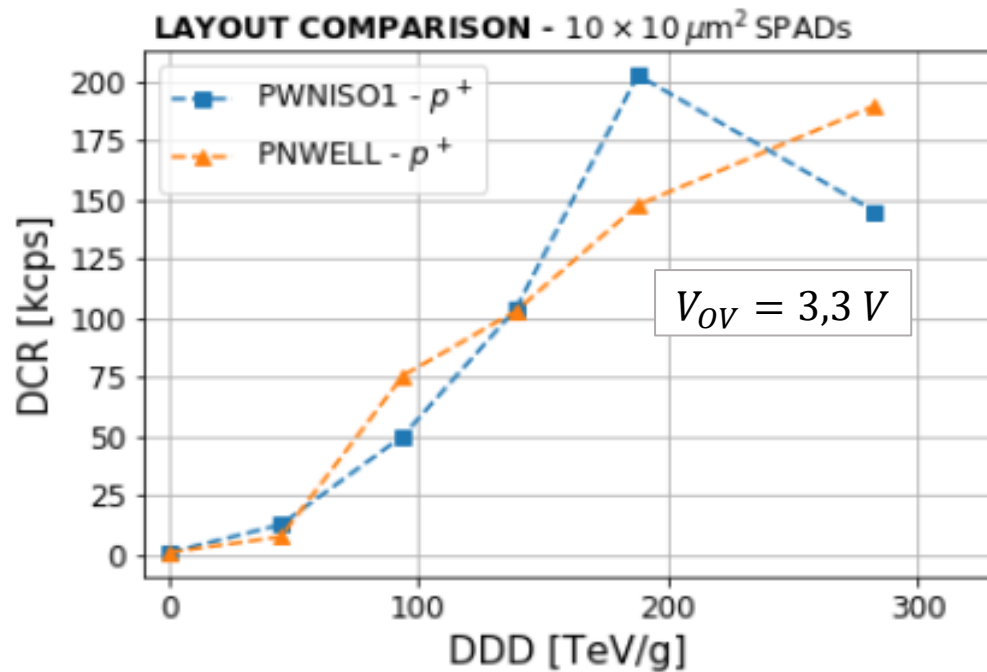


Claude Leroy, Pier-Giorgio Rancoita, "Principles of Radiation Interaction in Matter and Detection 2nd Edition", World Scientific Publishing, 2009.

# Protons irradiation effects

Mean DCR increases up to two order of magnitude at maximum dose delivered;

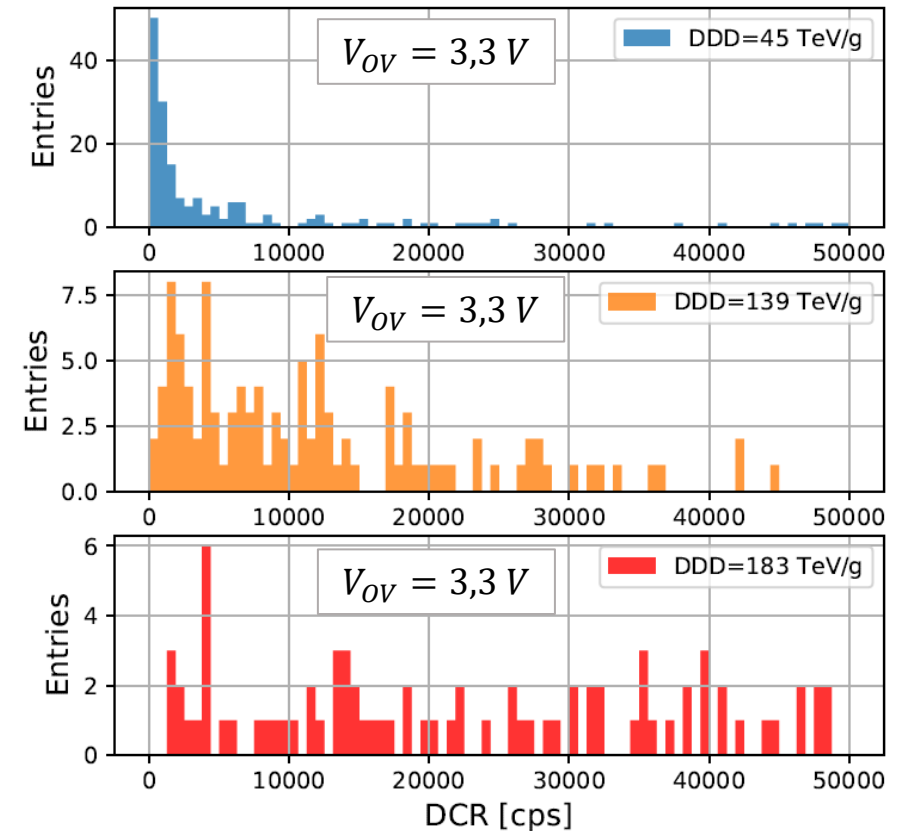
No relevant differences between PNWELL and PWNISO1/2 layouts.



$\frac{\Delta \text{DCR}}{\text{DDD}} \left[ \frac{\text{cps}}{\text{TeV} \cdot \text{g}} \right]$	PNWELL	PWNISO1	PWNISO2
	708	678	692

DCR increase factor from linear fit

**DCR distribution in PWNISO1 during irradiation**

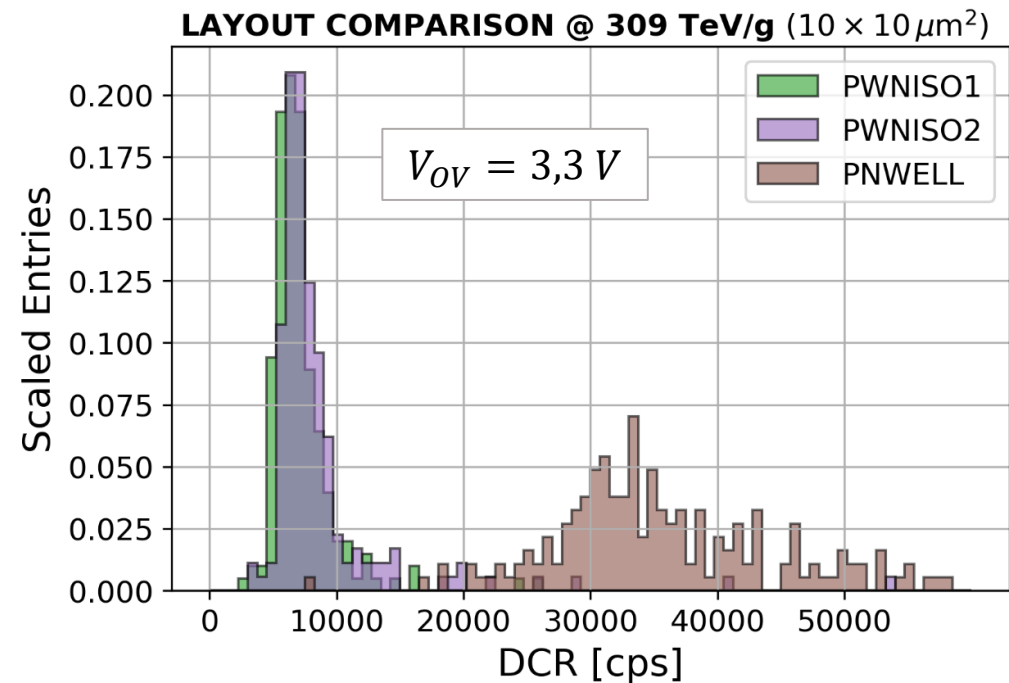
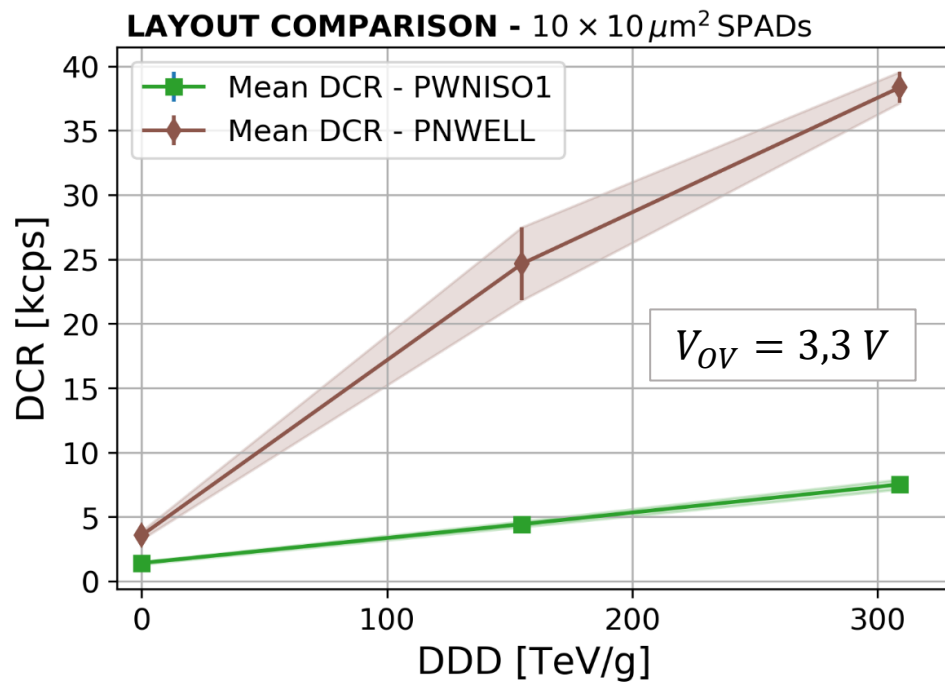




# Electron irradiations effects

PWNISO1 and 2 shows no significant differences: no role due to defects created in the STIs;

For the PNWELL the DCR increase is 5 time larger than in PWNISO1-2, beside the smaller active volume.



$\frac{\Delta \text{DCR}}{\text{DDD}} \left[ \frac{\text{cps}}{\text{TeV g}} \right]$	PNWELL	PWNISO1	PWNISO2
	112	19,8	20,1

DCR increase factor from linear fit

# DCR induced degradation: P/S analysis

Possible indications about the origin of the damage, i.e., ionization and/or displacement from P/S dependence analysis.

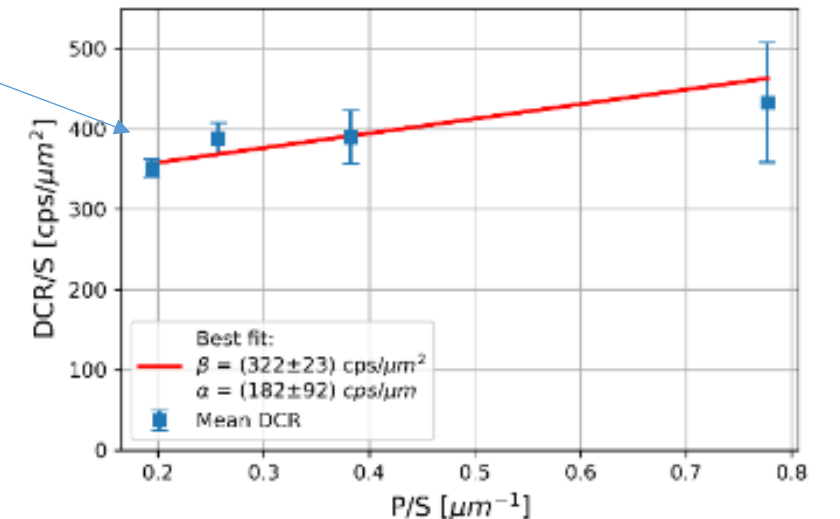
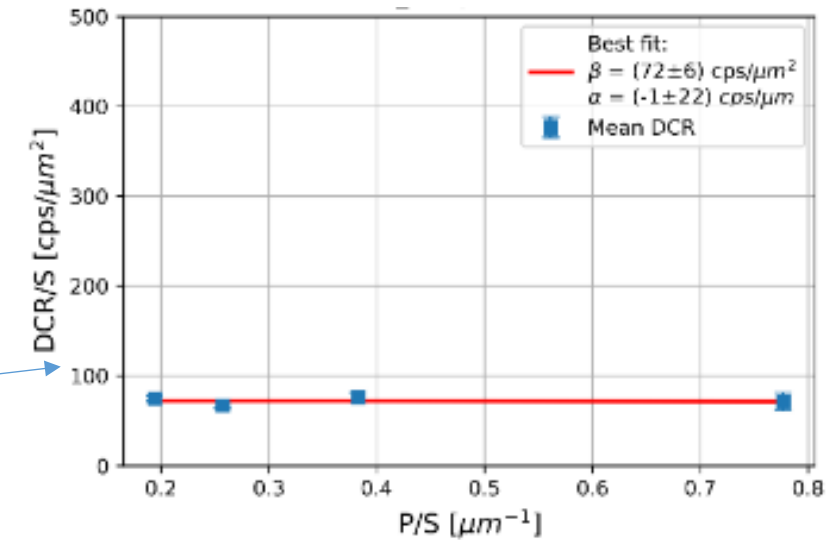
- TID effects expected at the perimeter of the SPAD, due to trapped interface states induced in the STI leads
- Non-ionizing effects expected from defects distributed in entire p-n depletion volume.

Only surface dependence in the PWNISO junction.

Some perimeter contribution observed in the PNWELL junction.

SPAD Layout	Optical Window [ $\mu\text{m}$ ]	Mean DCR [kcps]	Perimeter DCR [%]	Surface DCR [%]
PWNISO1	10	7.4	$\sim 0$	100
	20	29.6	$\sim 0$	100
PWNISO2	10	8.6	$\sim 0$	100
	20	31.3	$\sim 0$	100
PNWELL	10	37.9	18	82
	20	139.6	10	90

TABLE II. Dark Count Rate analysis on different SPAD structures irradiated at a displacement damage dose of 309 TeV/g.



# DCR induced degradation: NIEL scaling

Effects induced by 2 MeV and 16 MeV protons in comparison

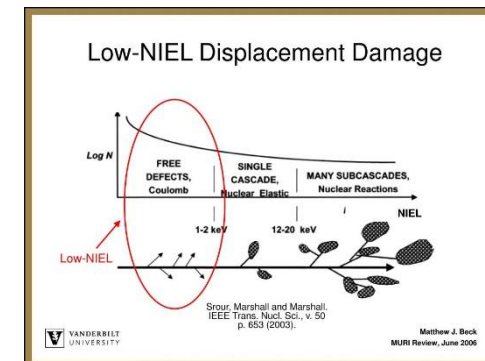
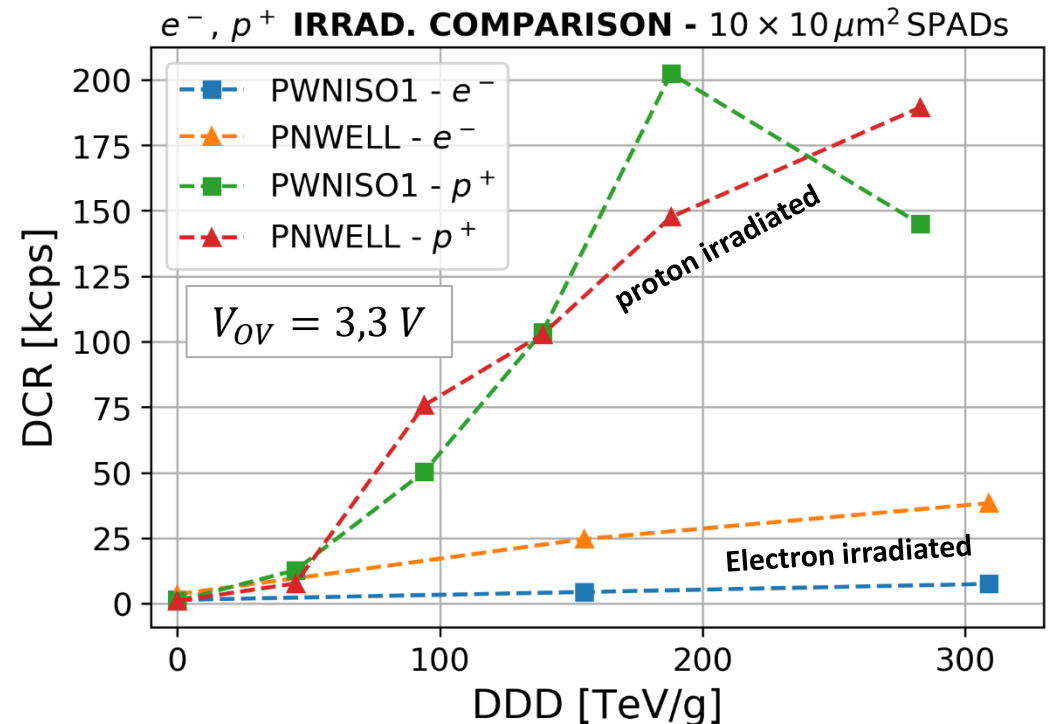
- **degradation after electron irradiation lower wrt proton irradiation**

Similar effects reported in literature for various devices. In [1] an effective NIEL for electrons has been proposed.

**Might depend on the induced defect type:**

- Low-Energy electrons produce mainly isolated defects (point-like defects).
- Protons produce defects relatively close together to form a local region of disorder (defect cluster).

[1] [P. Arnolda, et al., NIEL Scaling: Comparison With Measured Defect Introduction Rate in Silicon](#)

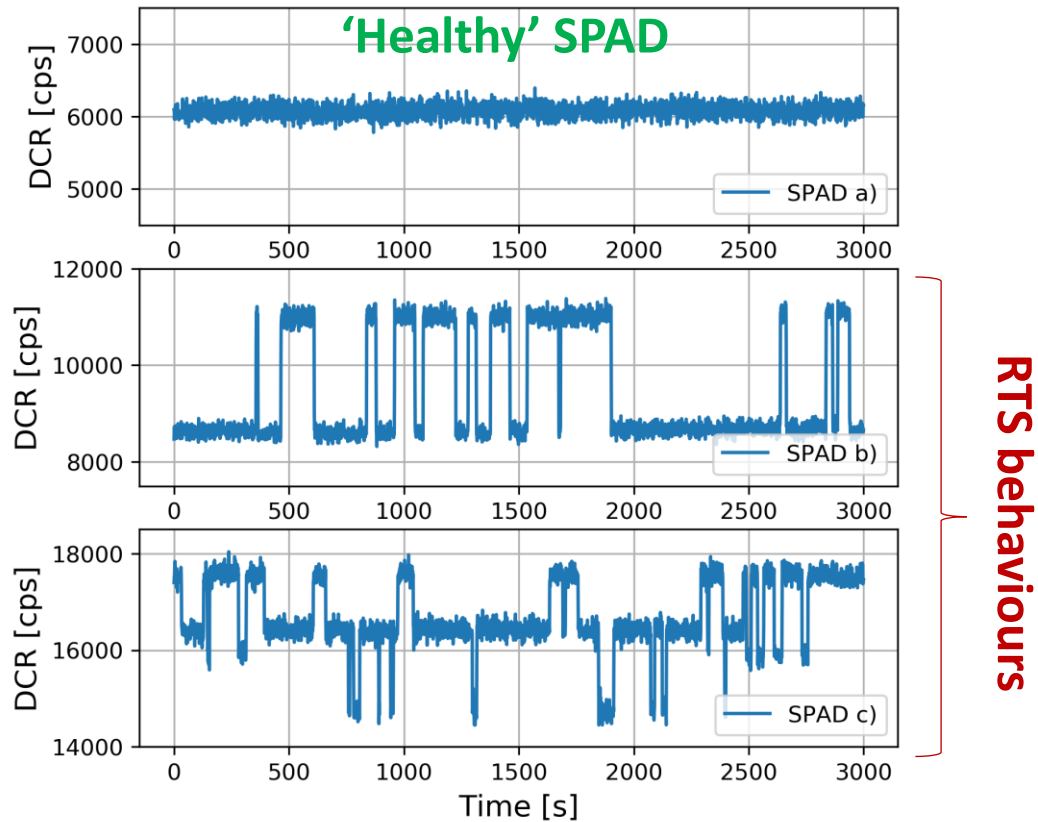


# Random Telegraph Signals observation

After irradiation discrete fluctuation of DCR between two or more levels have been observed.

This phenomenon is known in literature as **Random Telegraph Signal Noise**.

**DCR vs observation time**



Similarities to the RTS effects observed in MOS devices, at the origin of the flicker noise.

In MOS, due to charge trapping/detrapping in defects at SiO<sub>2</sub> interfaces

In SPADs, it is related to metastable defects located in the device bulk region.

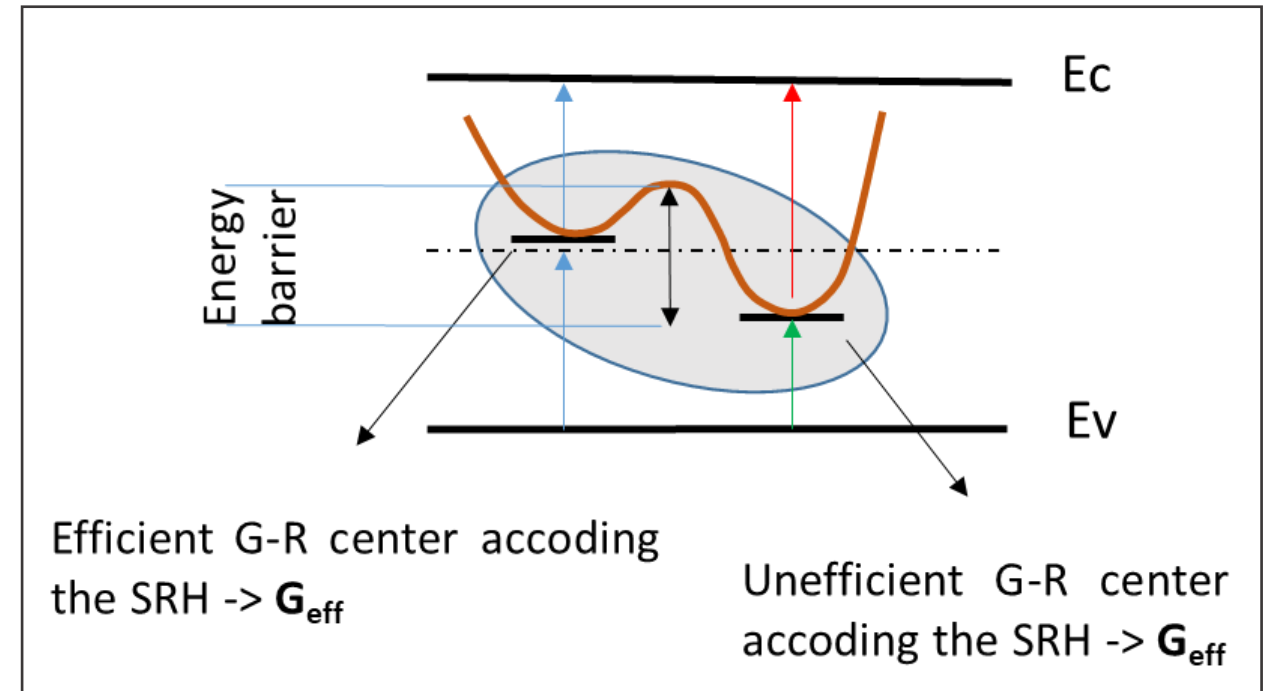
# Random Telegraph Signal: defects

In bulk devices RTS origin due to defects which exists in two or more stable configurations.

Metastable defects can randomly change their configuration:

- As a consequence, the  $e-h$  generation rate can change, resulting a 'jump' in the level of DCR.
- An energy barrier must be overcome to switch from one configuration to another: for this reason the RTS switching frequency is expected to depend on the temperature.

## Bi-stable complex defect schematization



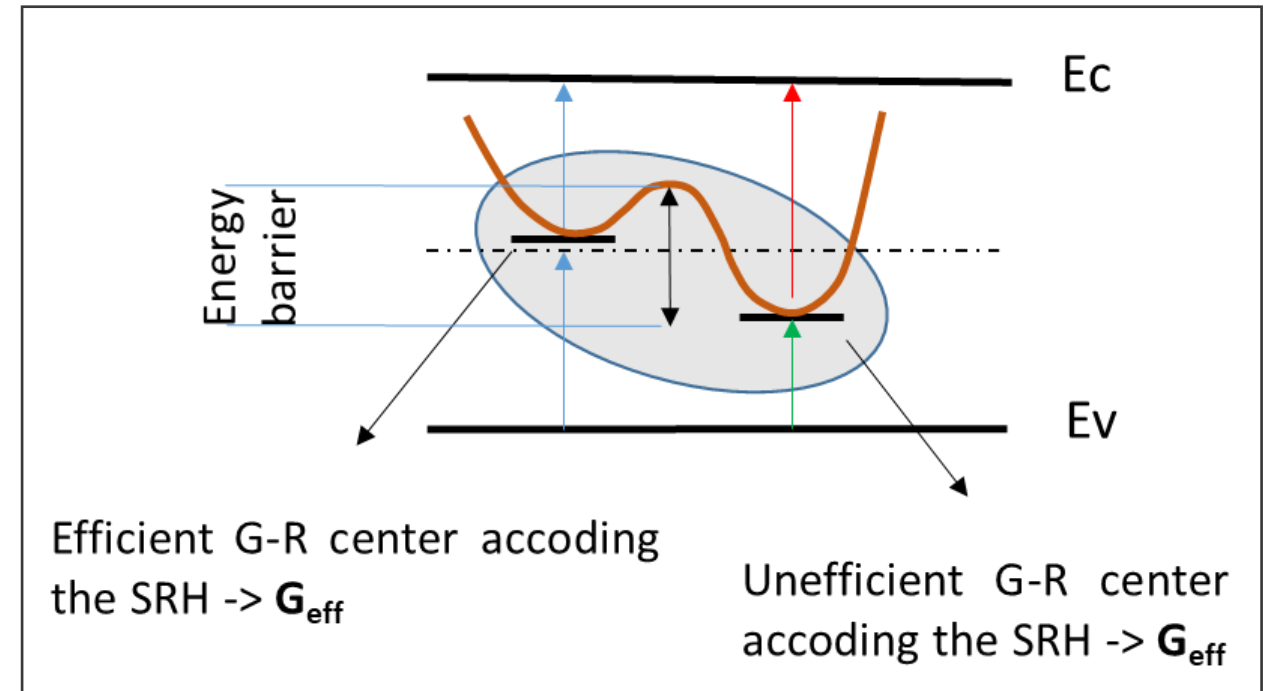
# Random Telegraph Signal: defects

In bulk devices RTS origin due to defects which exists in two or more stable configurations.

Possible sources:

- **Phosphorus-Vacancy (P-V) defects** have a dipole structure. The dipole axis can change with the vacancy position and may induce RTS. [G. D. Watkins and J. W. Corbett, 1964; H. Hopkins, G.R. Hopkinson, 1995, T. Nuns, 2007]
- The interaction of neutral **di-vacancies in cluster defects** can produce a reaction called “Inter-center transfer” which has the effect of increase the generation rate.

## Bi-stable complex defect schematization

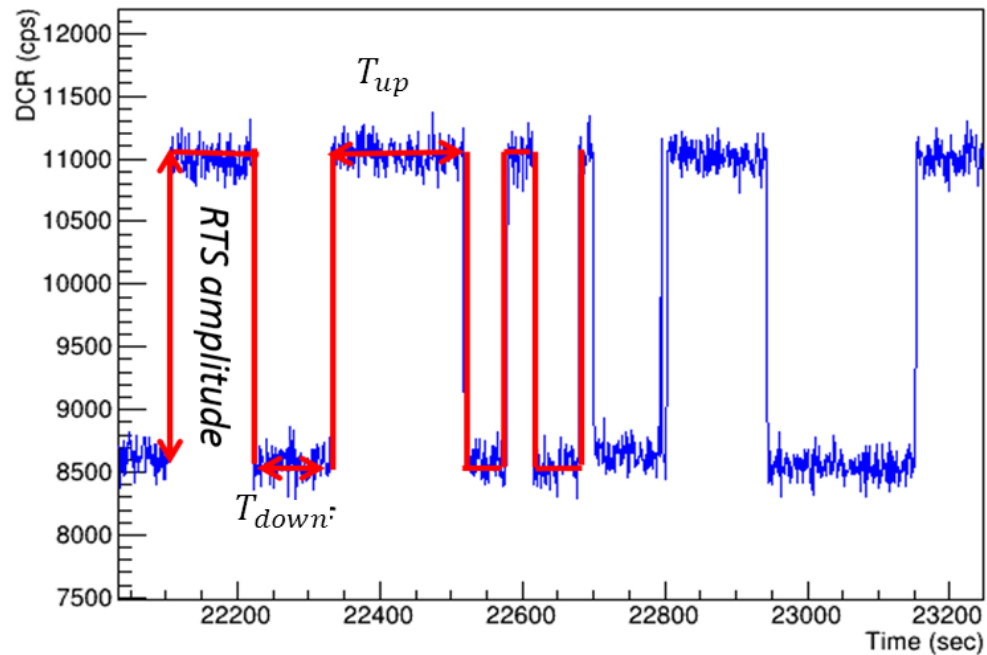


# RTS time analysis

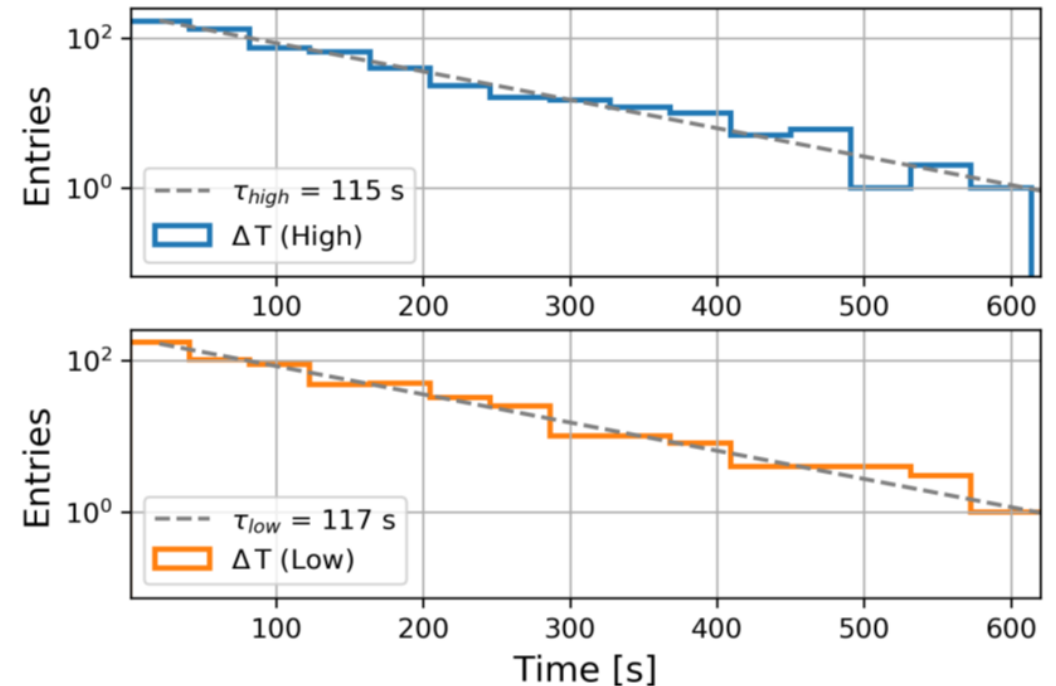
For the two-level case, RTS behaviours analysed as a function of observation time.

- Follow Poisson distribution law for random switching events.
  - Times between RTS transitions are exponentially distributed.

DCR vs observation time



Up/Down state time distribution

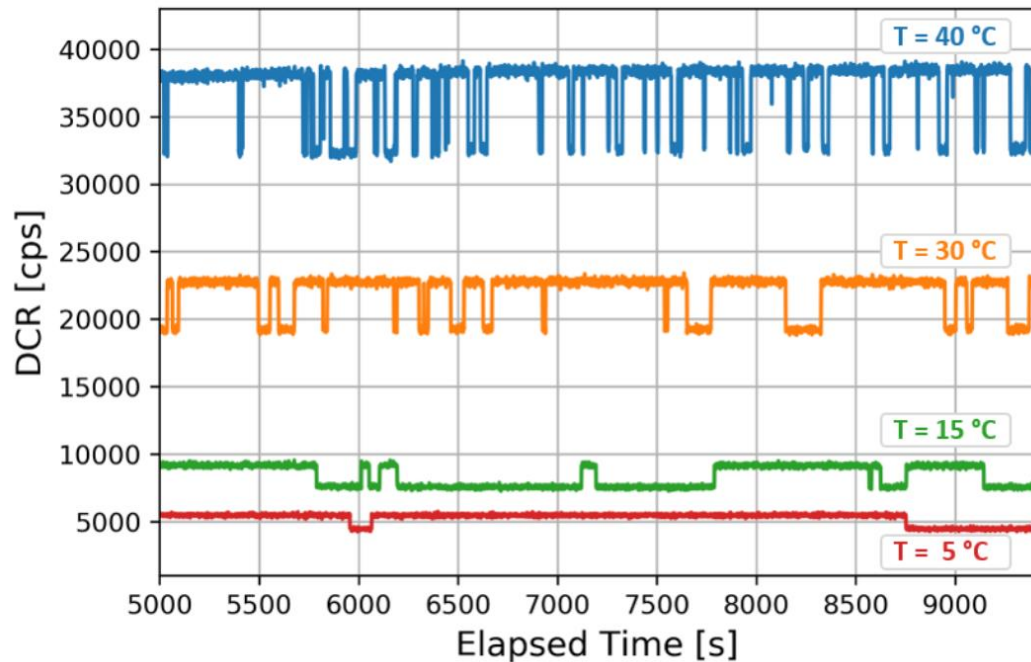


# RTS vs temperature

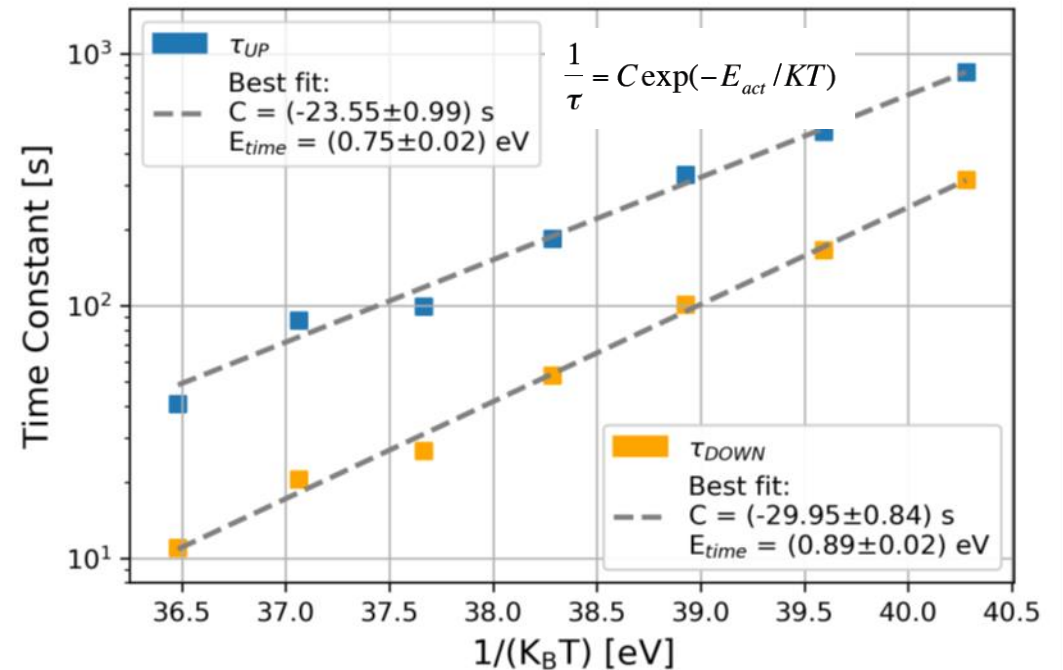
For the two-level case, RTS behaviours analysed as a function of temperature.

- RTS amplitude and switching probability increase with temperature, following an exponential dependence.

### RTS as a function on Temperature



### RTS time constant vs. Temperature



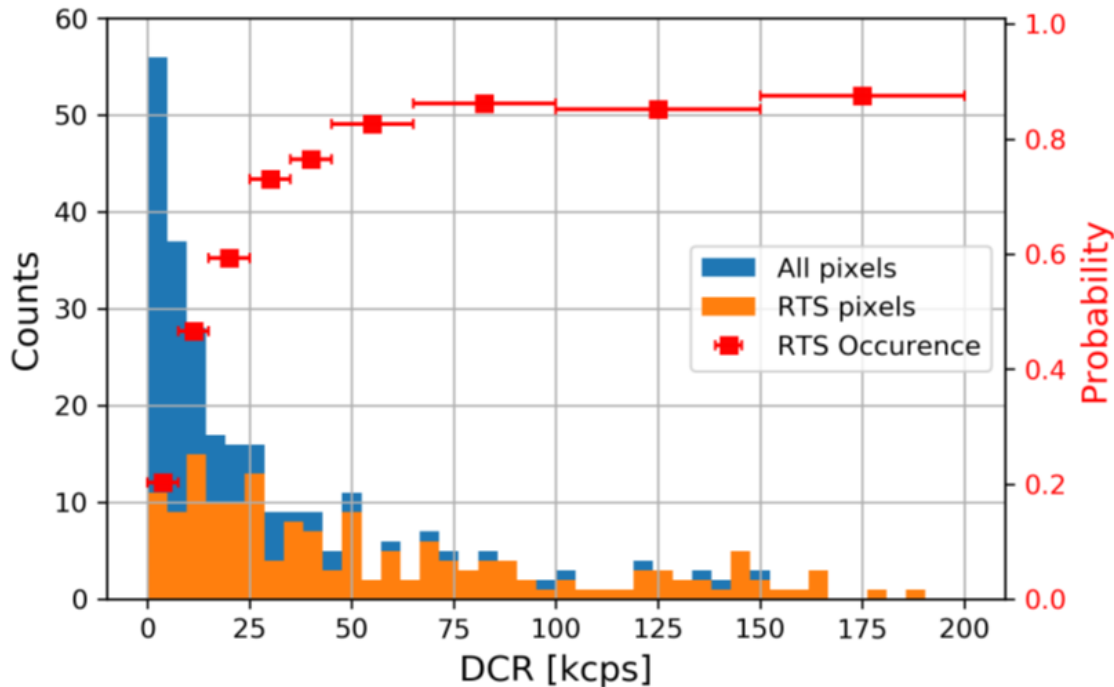


# RTS occurrence

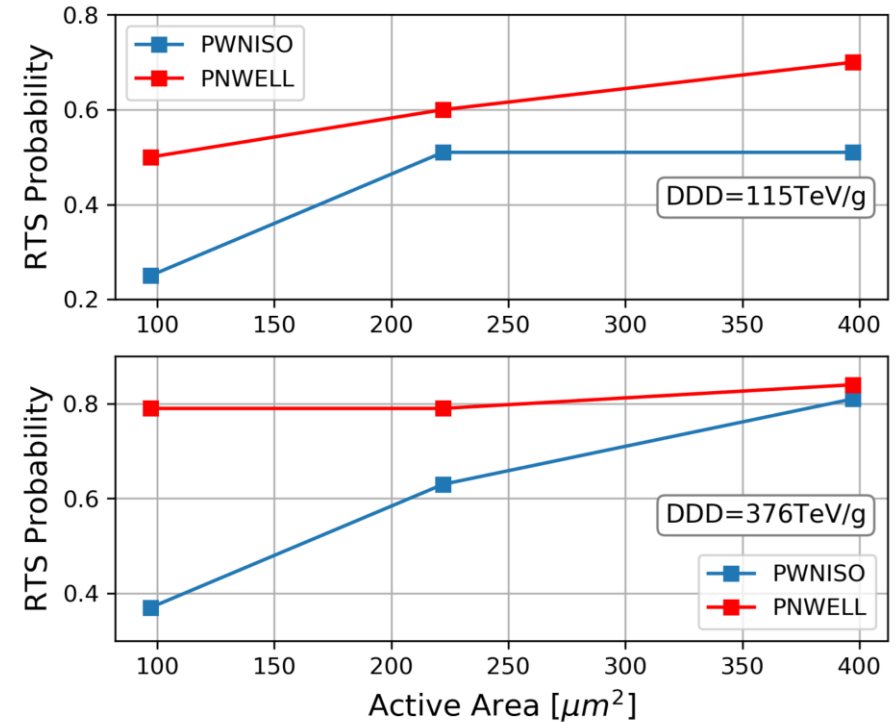
RTS occurrence studied for different SPAD layouts:

- higher probability to observe RTS occurrence for pixels that exhibit high DCR after irradiation.
- probability of having RTS increases with the SPAD sensitive area and with the DDD level.

RTS probability vs SPAD DCR



RTS probability vs SPAD area



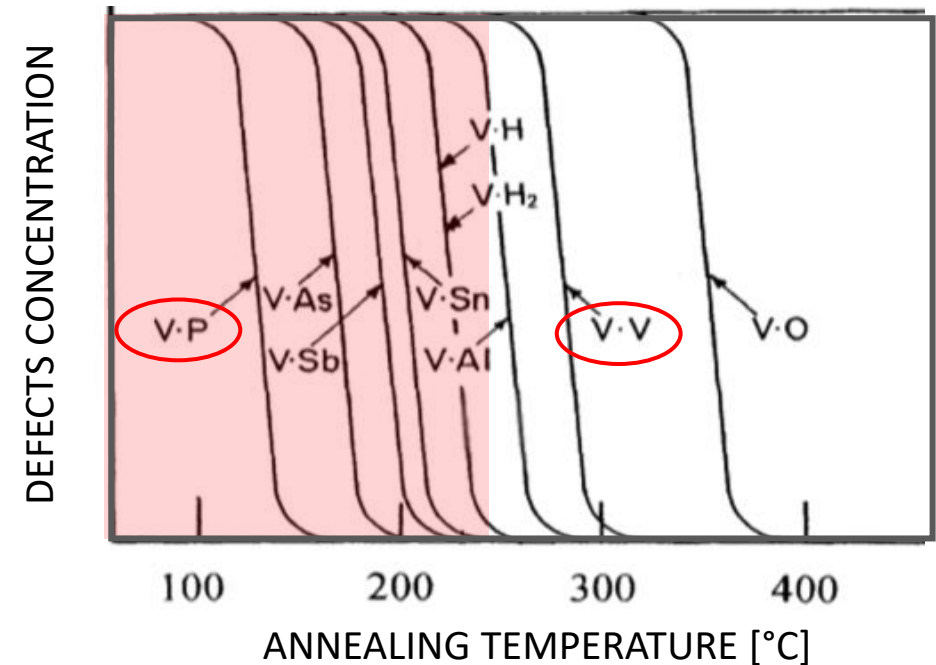
# Isochronal Annealing

The annealing procedure is a useful tool to investigate the defects responsible for DCR and RTS.

- Different bound energy of the defects results in different annealing temperature:
  - P-V centers anneal at about 130°C
  - Di-Vacancies anneal at 270°C

Our results suggest the P-V complex defects as a candidate responsible for DCR increase and Random Telegraph Signal behaviour.

Schematic of vacancy-defect annealing \*

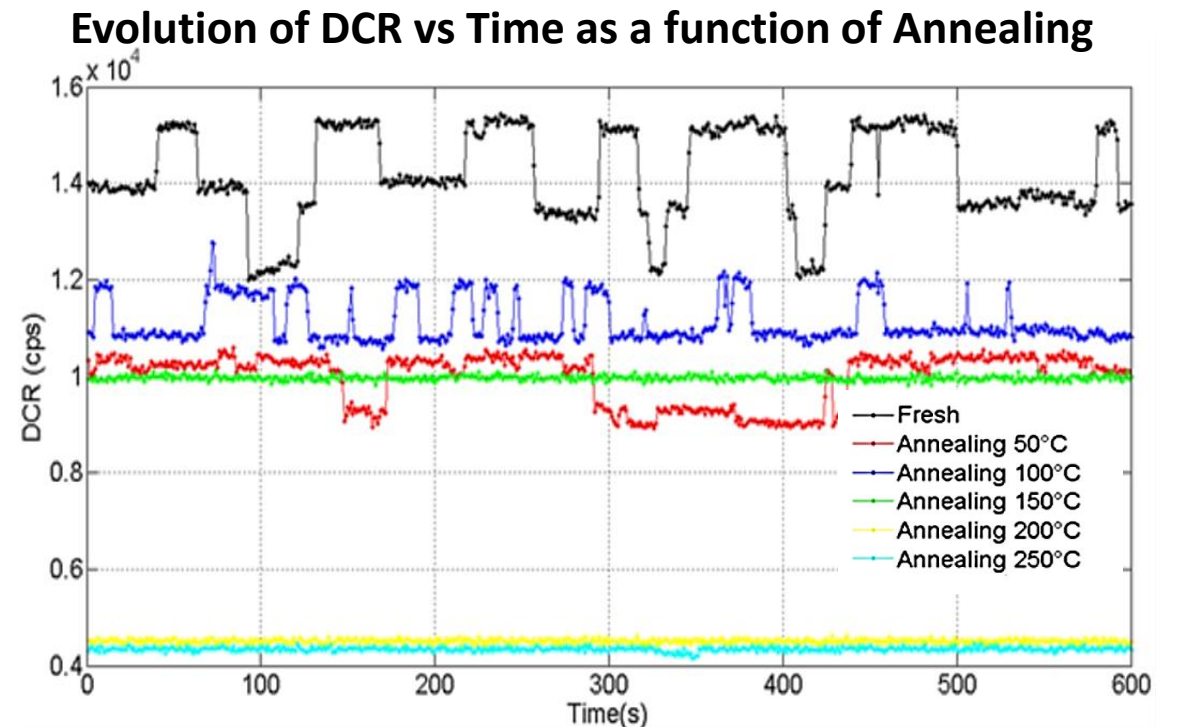
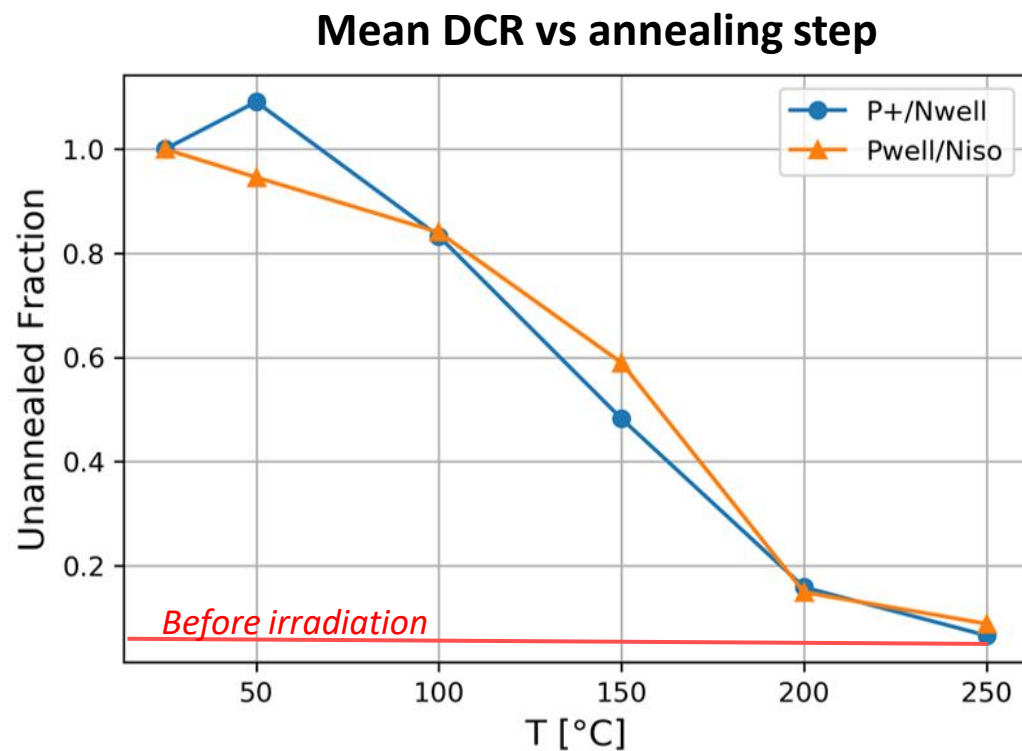


\*"Annealing of Proton-Induced Random Telegraph Signal in CCDs", T. Nuns et al.

# Isochronal Annealing

DCR of irradiated SPAD has been measured after several annealing steps between 50°C and 250°C.

- After annealing the mean DCR recovered its initial value, while multi-level RTS transformed into lower level and less frequent RTS, before completely disappear.



# Backup

# References

[“Proton induced dark count rate degradation in 150-nm CMOS single-photon avalanche diodes”, M. Campajola et al.](#)

[“Random Telegraph Signal in Proton Irradiated Single-Photon Avalanche Diodes”, F. Di Capua et al.](#)

# Random Telegraph Noise

- Phosphorus-Vacancy (P-V) defects can be generated in doped silicon devices. It can be formed at any of four Si-atoms around the P-atom.
- P-V center has a dipole structure. The dipole axis can change with the vacancy position and may induce RTS.
- Calculation on kinetics of reorientation predicts 0.9 eV for activation energy. [G. D. Watkins and J. W. Corbett, 1964; H. Hopkins, G.R. Hopkinson, 1995, T. Nuns, 2007]

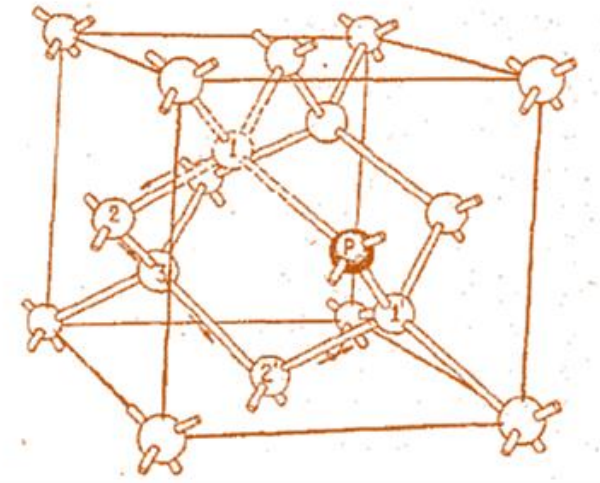


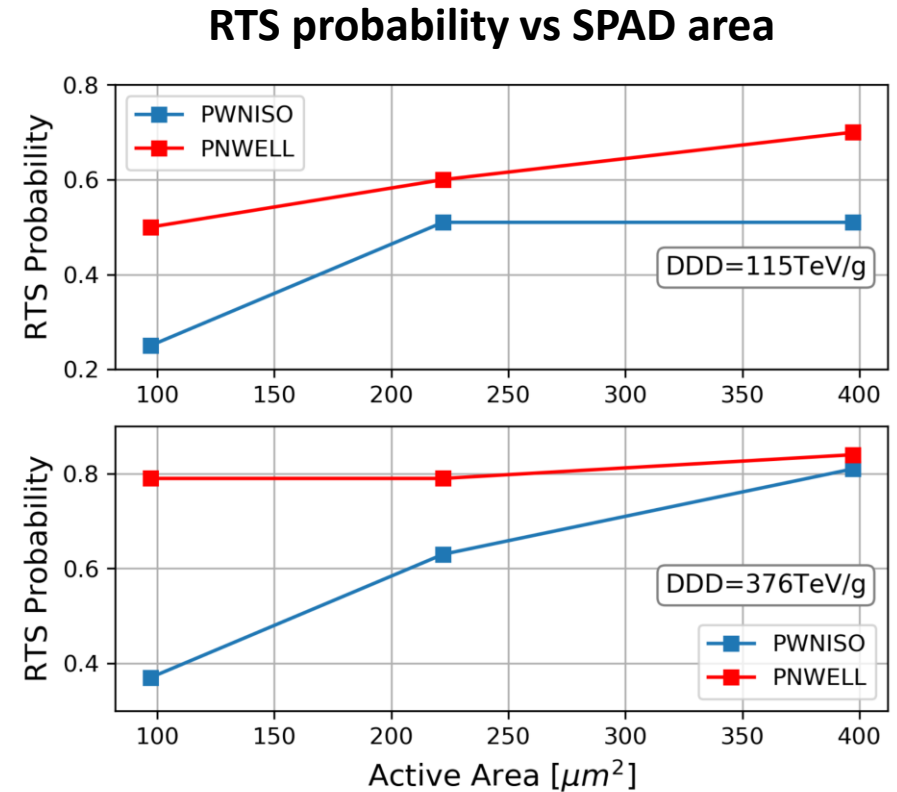
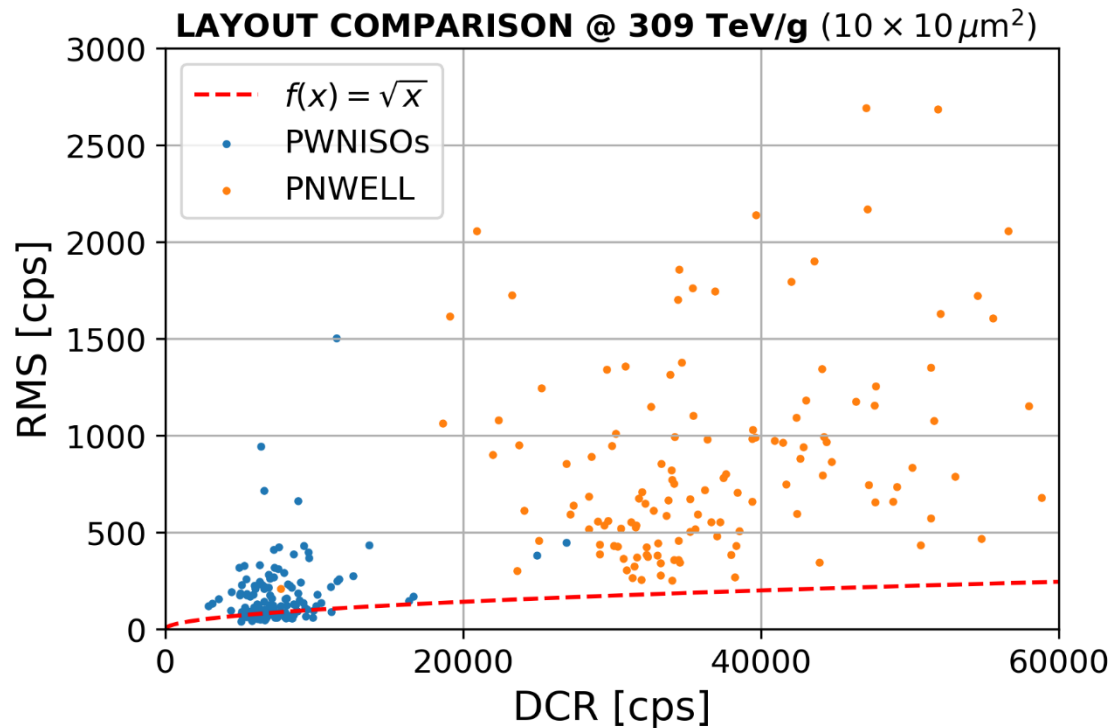
Figure from Watkins & Corbett (1964)

- Di-Vacancies cluster: these defects have three energy levels and four charge states (+,0,-,2-).
- The interaction of neutral di-vacancies (the most probable state) can produce a reaction called “Inter-center transfer” which has the effect to increase the generation rate.
- The rearrangement of defects can create configuration in which inter-center transfer is possible and in other no, giving rise to RTS.

# RTS occurrence

RTS occurrence studied for different SPAD layouts:

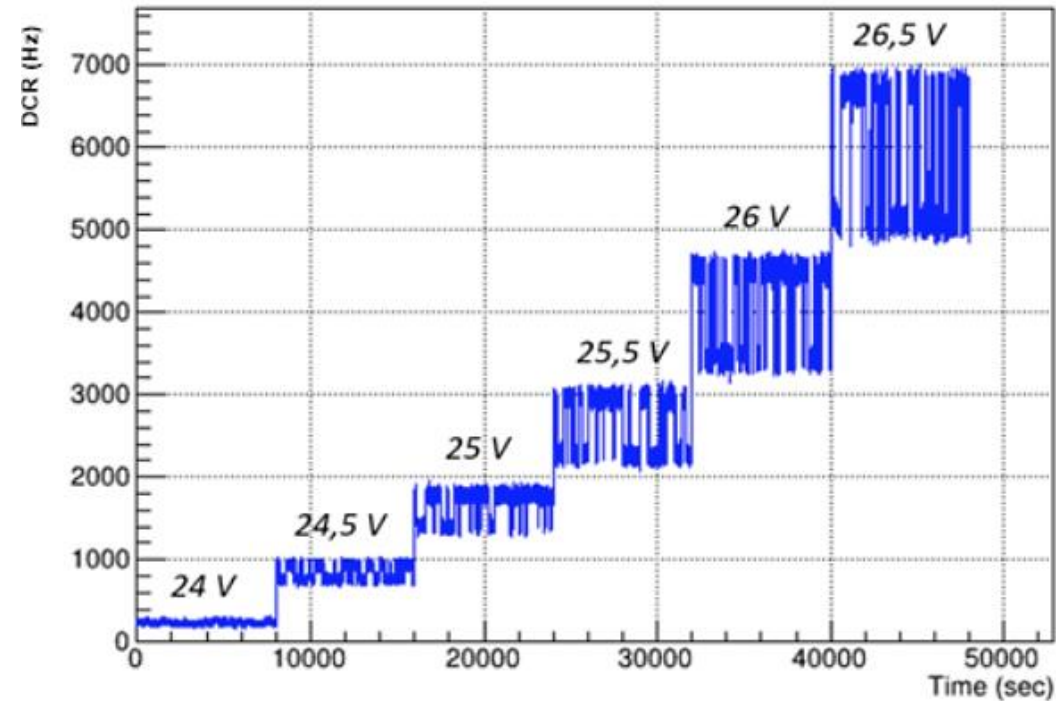
- higher probability in PN junctions



# Random Telegraph Noise

- RTS amplitude increase with the overvoltage

RTS amplitude vs overvoltage



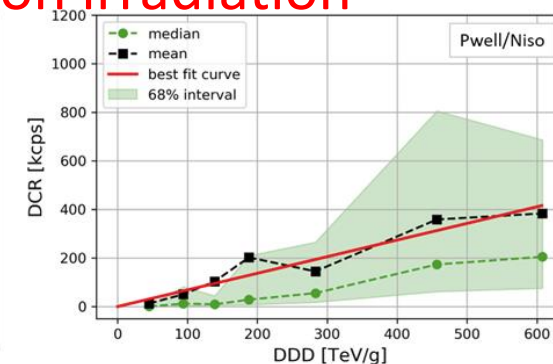
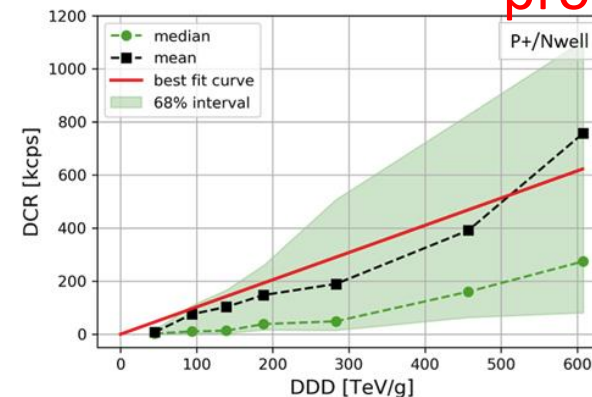


# Radiation damage studies

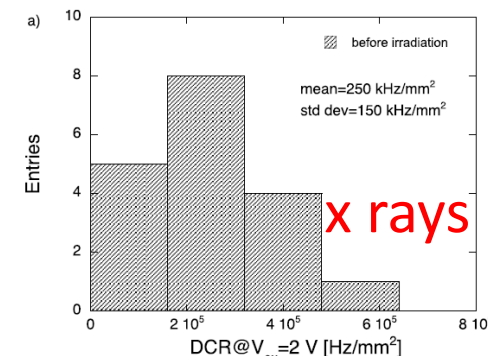
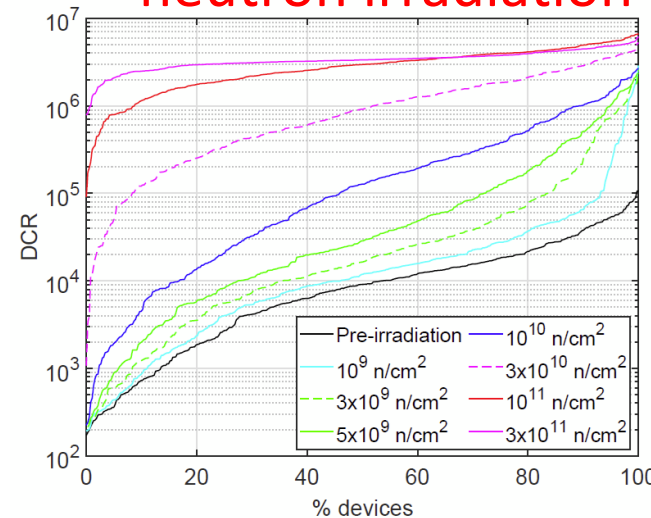
Large degradation observed in previous studies [1]:

- First 150 nm devices -> few MHz/mm<sup>2</sup>
  - $\sim$  GHz/mm<sup>2</sup> at 10<sup>10</sup> p/cm<sup>2</sup>
- APIX 180 nm devices: 1 MHz/mm<sup>2</sup> [2,3,4]
  - $\sim$  GHz/mm<sup>2</sup> at 10<sup>11</sup> n<sub>eq</sub>/cm<sup>2</sup>
  - +30% DCR increase with 1 Mrad

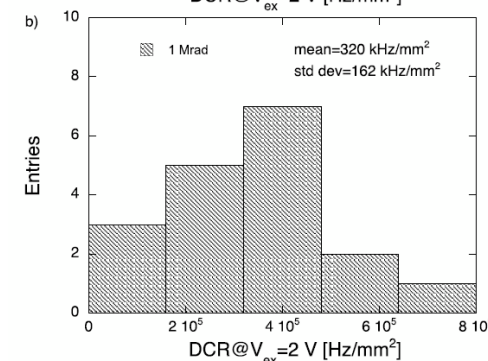
proton irradiation



neutron irradiation



x rays

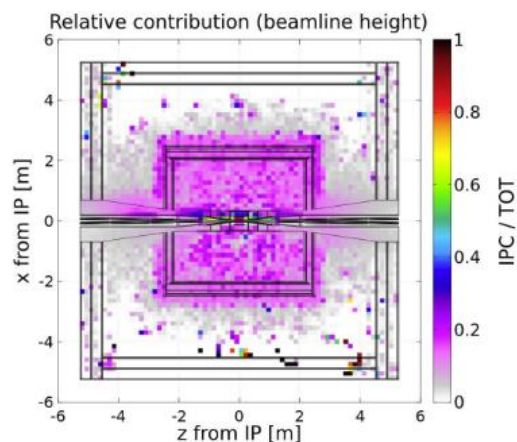
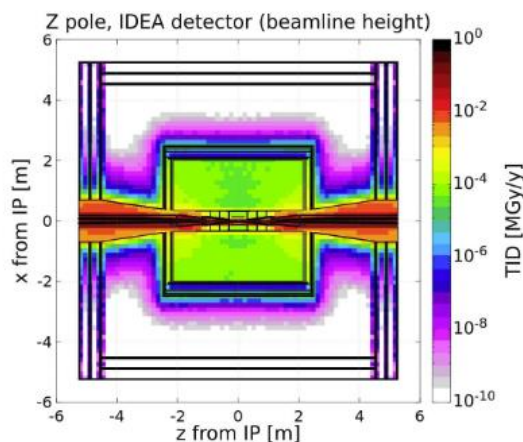


[1] M. Campajola, et al., Proton induced dark count rate degradation in 150-nm CMOS single-photon avalanche diodes, NIMA  
 [2] M. Musacci, et al. "Radiation tolerance characterization of Geiger-mode CMOS avalanche diodes for a dual-layer particle detector." NIMA  
 [3] L. Ratti, et al. "Dark Count Rate Degradation in CMOS SPADs Exposed to X-Rays and Neutrons" TNS  
 [4] A. Ficorella, APPLICATION OF AVALANCHE DETECTORS IN SCIENTIFIC AND INDUSTRIAL MEASUREMENT SYSTEMS, PhD thesis

## IDEA radiation levels (RB + IPC)

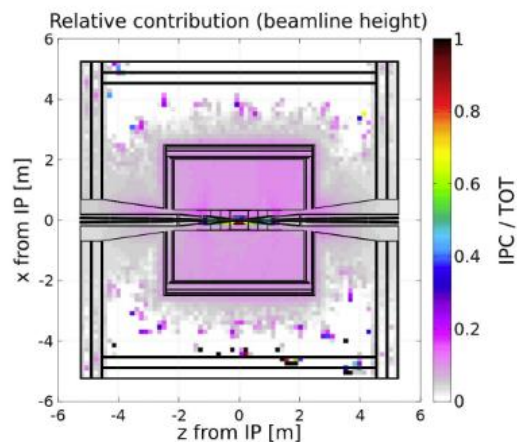
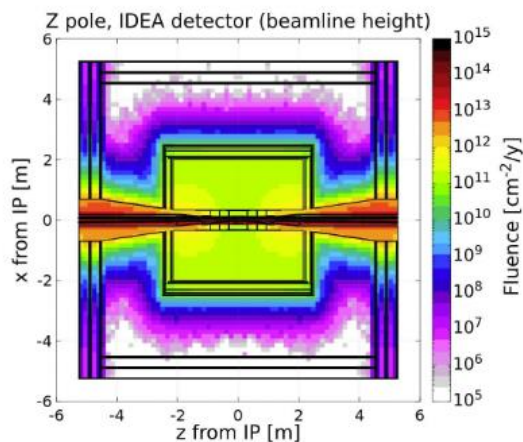
**incomplete magnetic field map:**  
results will be altered, to be revisited  
with the a map covering the full detector

Dose



- Drift chamber: 100 Gy/year
- Calorimeter: <10 Gy/year
- RB dominates
- IPC contributes up to 20% in the drift chamber

Fluence



- Drift chamber:  $10^{11}$  cm<sup>-2</sup>/year
- Calorimeter: < $10^{10}$  cm<sup>-2</sup>/year
- RB dominates
- IPC contributes up to 10% in the drift chamber